Submitted to

International Europhysics Conference on High Energy Physics, EPS03, July 17-23, 2003, Aachen
(Abstract **107** Parallel Session **5**)

XXI International Symposium on Lepton and Photon Interactions, LP03, August 11-16, 2003, Fermilab

www-h1.desy.de/h1/www/publications/conf/conf_list.html

Measurements of the Inclusive Photoproduction of η, ρ^0, $f_0(980)$ and $f_2(1270)$ Mesons at HERA

H1 Collaboration

Abstract

Measurements are presented of the inclusive photoproduction of the neutral mesons η, ρ^0, $f_0(980)$ and $f_2(1270)$ in ep interactions at HERA at an average γp collision energy of 210 GeV. Inclusive cross-sections are shown differentially as a function of various kinematic variables and a comparison is made with measurements of the photoproduction of other particle species at HERA.

1 Introduction

The process by which quarks and gluons convert to colourless hadrons is one of the outstanding problems in particle physics. The theory of perturbative quantum chromodynamics (QCD) is not applicable and phenomenological models based on the laws of thermodynamics are often used [1–3]. High energy particle collisions which give rise to large multiplicities of particles produced with low values of transverse momentum provide an opportunity to study hadronisation. This paper presents precision measurements made by the H1 experiment of the inclusive photoproduction of various species of neutral mesons in ep collisions at HERA.

Although the production of long-lived hadrons and hadronic resonances has been studied in detail at LEP in Z decays [4], measurements made in high energy hadronic collisions are sparse. In hadronic collisions it has been found that particle production at central values of rapidity is independent of the type of the colliding hadrons and is governed by the fundamental properties of the QCD vacuum. In heavy ion collisions phase transitions can take place to give states in which quarks become free to move about within a confinement volume much larger than the volume of a typical hadron (Quark-Gluon Plasma). These phase transitions also result in a change in the properties of the hadronic final state. Such measurements are presently being carried out at RHIC in heavy ion collisions at $\sqrt{s_{NN}} = 200$ GeV. It is therefore important to study particle production in light hadron collisions at about the same energy. This is possible at the H1 experiment at the HERA collider which so far has collected millions of multihadronic photoproduction events. Measurements of the inclusive photoproduction of charged particles [5], long-lived hadrons like K^0_S mesons, Λ^0 baryons [6] and charmed mesons [7] have already been reported by the H1 and ZEUS collaborations. The particle spectra measured at HERA are found to display interesting regularities [8].

In this report, the first measurements of the inclusive photoproduction of the neutral hadronic resonances η, ρ^0, $f_0(980)$ and $f_2(1270)$ at HERA are presented. The measurements are based on about four million multihadronic events recorded by the H1 detector at an average photon-proton centre-of-mass energy $W = 210\,\text{GeV}$ in the 2000 running period which correspond to an integrated luminosity of $38.7\ \text{pb}^{-1}$.

2 H1 detector

The H1 detector is described in detail elsewhere [9]. A brief account of the components that are most relevant to the present analysis is given here. These are the positron tagger, the central tracker and the liquid argon (LAr) calorimeter. The direction of the z-axis is chosen to be along the proton beam direction and the polar angle θ is defined with respect to this axis. The variables rapidity and pseudorapidity are defined by $y = \frac{1}{2}\ln\frac{E+p_z}{E-p_z}$ and $\eta = -\ln(\tan(\theta/2))$, respectively.

The positron tagger, located at 33 m from the interaction point in the positron direction, measures the energy of the scattered positron and, in conjunction with the photon detector, the luminosity by exploiting the Bethe-Heitler process $ep \to e'p'\gamma$. The photon detector is located 100 m from the interaction point, in the positron direction.

The central track detector consists of the central jet chamber (CJC), multi-wire proportional chambers for triggering purposes and two additional drift chambers which measure accurately the z-coordinates of charged particle tracks. The pseudorapidity range covered by the central track detector is $|\eta| < 1.5$. The CJC has 56 sensitive wire layers and is placed inside a uniform magnetic field of strength 1.15 T. The CJC measures the transverse momentum of charged particles with a resolution of $\sigma_{p_T}/p_T \approx 0.009 \times p_T[\text{GeV}] \oplus 0.015$.

The LAr calorimeter surrounds the tracking system and covers the angular range $4^\circ < \theta < 154^\circ$. The calorimeter is used here for photon reconstruction.

Photoproduction events are selected by requiring the presence of a scattered positron in the small angle positron tagger. For these events the photon virtuality is restricted to $Q^2 < 10^{-2}\,\text{GeV}^2$. The energy measured by the positron tagger is used in the determination of the total γp collision energy, W. In the main detector, γp events are triggered by demanding the presence of at least three tracks in the CJC in addition to a signal in the positron tagger.

3 Event selection

In order to reduce the non-ep background contamination and to ensure good reconstruction of the event kinematics, the following selection criteria are applied in this analysis:

- Photoproduction events are required to lie within the interval $174 < W < 256$ GeV. This corresponds to an average photon-proton collision energy of $W = 210\,\text{GeV}$.
- The trigger conditions are verified by selecting only multi-hadron events with more than two reconstructed tracks pointing to the common event vertex.
- In order to suppress random coincidences between Bethe-Heitler events, which occur at a high rate, and beam-gas background in the main H1 detector, events are rejected if a photon with energy $E_\gamma > 2\,\text{GeV}$ is detected in the photon tagger.
- The event vertex reconstructed from the tracks of charged particles is required to lie within $\pm 35\,\text{cm}$ of the nominal z-position of the interaction point, corresponding to about a 3σ cut on the length of the interaction region which is defined by the longitudinal size of the proton bunch.

In total about 3.7×10^6 events satisfy the above selection criteria.

The extraction of cross sections from the observed event rates requires the detailed simulation of the response of the H1 detector to photoproduction interactions. The PYTHIA 6.1 Monte Carlo (MC) event generator [10] is used to simulate multihadron events resulting from photon-proton interactions. The hadronisation process is modelled using the LUND string fragmentation scheme (JETSET [11]). The photoproduction events generated by PYTHIA are passed through a simulation of the H1 detector based on GEANT [12] and then through the same reconstruction and analysis chain as used for the data.

4 Inclusive cross section determination

4.1 The η meson cross section

The η mesons are reconstructed via their two-photon decay mode. The photons are identified as isolated LAr calorimeter clusters with energy greater than $200\,\mathrm{MeV}$ and polar angle in the range $0.5 < \theta < 2.6$. More than 90% of the cluster energy is also required to be contained in the electromagnetic section of the LAr calorimeter. Figure 1c) shows the energy distribution of the clusters which satisfy these requirements. It is reasonably described by the MC simulations.

The transverse radius of an electromagnetic cluster about the axis of the shower, R_{tr}, is defined using the expression:

$$R_{tr} = \frac{1}{A}\sum_i \frac{E_i r_i^2}{V_i}, \qquad \text{with} \qquad A = \sum_i \frac{E_i}{V_i}\,,$$

where E_i and V_i are the energy and volume of the i^{th} LAr calorimeter cell in the cluster and r_i denotes the radial distance of the cell from the shower axis. The R_{tr} distribution for the selected event sample is shown in figure 1d). The tail at large values of R_{tr} is caused by hadrons absorbed in the LAr calorimeter. To separate the genuine electromagnetic clusters from clusters produced by hadrons, R_{tr} is required to be smaller than $8\,\mathrm{cm}$.

In addition, clusters associated with charged tracks are rejected. Figure 1e) shows the distribution of the distance between the cluster centre and the closest reconstructed charged track, D_{CT}. The peak at low D_{CT} values corresponds to clusters associated with charged particles. To reduce this background, D_{CT} is required to be larger than $15\,\mathrm{cm}$.

Since η mesons decay isotropically, the distribution of the cosine of the angle α between the photon's momentum in the meson rest frame and the direction of the meson in the γp rest frame is expected to be flat. Conversely, the combinatorial background is expected to be strongly anisotropic. The distribution of $|\cos(\alpha)|$ is shown in figure 1f). To reduce the combinatorial background, the requirement that $|\cos(\alpha)| < 0.7|$ is made.

The reconstruction efficiency for η mesons is calculated using the Monte Carlo simulation described above. This efficiency is about 30% for η mesons with transverse momenta below $8\,\mathrm{GeV/c}$. Above this value, the two clusters in the LAr calorimeter produced by the η decay photons start to merge. For η mesons with transverse momentum below $3\,\mathrm{GeV/c}$, the large combinatorial background precludes a reliable identification of the signal. Therefore, the kinematical interval chosen for the η meson cross section measurements is restricted to $3 < p_T < 8\,\mathrm{GeV/c}$.

In figure 2 the spectrum of the invariant mass of the photon pairs is shown. This mass spectrum is fitted using the sum of a Gaussian function for the η meson signal and a polynomial to describe the combinatorial background. In the fit, the nominal resonance mass is fixed to the Particle Data Group (PDG) value, while the width is fixed to the value obtained in the MC calculation.

To obtain differential cross sections, the data sample is divided into two intervals of rapidity and of transverse momentum. The fit procedure is applied in each bin separately. The first part

of the uncertainty on the cross section values represents the statistical error of the fit and is about 15%. The second part represents the systematic uncertainty. The major sources of systematic error are the variation of the assumptions about the combinatorial background shape in the fit procedure (11%), the uncertainty in the detector acceptance and efficiency calculations (9%), and the precision of the luminosity measurement (2%).

4.2 The ρ^0, $f_0(980)$ and $f_2(1270)$ meson cross sections

The ρ^0, $f_0(980)$ and $f_2(1270)$ mesons are reconstructed through their $\pi^{\pm}\pi^{\mp}$ decay mode. Any charged track found in the CJC with $p_T > 0.15$ GeV/c and polar angle $0.5 < \theta < 2.6$ is taken as a charged pion candidate. This limits the kinematical interval for the reconstructed neutral mesons in rapidity space to be $|y_{lab}| < 1$. The multiplicity and polar angle distributions of the selected charged tracks are shown ion figures 1a) and 1b), respectively. They are reasonably described by the MC simulation.

To extract the ρ^0, f_0 and f_2 signals, the two-particle invariant mass spectrum for like-sign pions $m(\pi^{\pm}\pi^{\pm})$ is subtracted from the spectrum of for opposite-sign pions $m(\pi^{\pm}\pi^{\mp})$. The resulting distribution is shown in figure 3, where the ρ^0, f_0, and f_2 signals are clearly seen above the residual combinatorial background.

In order to extract a cross section for a given meson, the subtracted invariant mass distribution is fitted using a function composed of three parts,

$$Fit(m) = BG(m) + \Sigma(BW(m)) + \Sigma(Ref(m))\,,$$

corresponding to the combinatorial background, signal and reflection contributions respectively. The combinatorial background term, $BG(m)$, is taken to have the form

$$BG(m) = a_1(m - 2m_\pi)^{a_2} e^{-a_3 m - a_4 m^2}$$

where m_π is the charged pion mass. The signal function describes three resonances,

$$\Sigma(BW(m)) = BW_{\rho^0}(m) + BW_{f_0}(m) + BW_{f_2}(m)\,,$$

where $BW(m)$ is the relativistic Breit-Wigner function,

$$BW(m) = A\frac{m_0 m\Gamma(m)}{(m^2 - m_0^2)^2 + m_0^2\Gamma^2(m)}\,,$$

with $\Gamma(m) = \Gamma_0 \left(\frac{q}{q_0}\right)^{2l+1} \frac{m_0}{m}$, and $l = 0$ for the f_0, $l = 1$ for the ρ^0, and $l = 2$ for the f_2 meson. The momentum of the decay products in the rest frame of their parents is q, and q_0 is the decay momentum when $m = m_0$, the nominal resonance mass. In the fit procedure the resonance masses remain as free parameters while their widths are fixed to the Particle Data Group (PDG) values. For the $f_0(980)$, the width is only poorly known and is hence allowed to vary from 50 to 100 MeV. The results should be taken as model-dependent measurements, which assume no interference of the f-signals with the background and no contribution to the f-meson peaks from $\pi^+\pi^-$ decays of other resonances at similar masses.

The third term, $\Sigma(Ref(m))$, represents the sum of the reflections in the two-pion mass spectrum originating from other resonance decays. Two major reflections contribute to the mass region of interest:

- a reflection from the decay $K^*(982) \to K^\pm\pi^\mp$ when the $K^\pm$ is misidentified as a charged pion;
- a reflection from the decay $\omega(782) \to \pi^\pm\pi^\mp\pi^0$ when the π^0 is not observed.

The shape of the reflection contributions is taken from the MC calculations and their normalization with respect to the ρ^0 signal is allowed to vary within broad intervals

$$\frac{N_{K^{*0}+\tilde{K}^{*0}} Br(\pi^\pm K^\mp)}{N_{\rho^0}} = 0.35 \pm 0.25 \qquad \frac{N_\omega}{N_{\rho^0}} = 1.0 \pm 0.2\,.$$

These cover the corresponding particle production ratios measured at hadron colliders [13] and in e^+e^- annihilation [14].

Figure 3 shows the result of the fit made in the mass range from 0.55 to $1.7\,\mathrm{GeV/c^2}$. The contribution of the reflections is also shown. The ρ^0 resonance in the data is shifted towards low mass. A similar effect has been reported by the LEP experiments [15]. It was conjectured that this arises as a result of final state interactions between the resonance and incoherently produced pions [16].

In order to calculate the meson production cross sections, detector acceptances and efficiencies are calculated using a Monte Carlo simulation of ρ^0 mesons. The $f_0(980)$ and $f_2(1270)$ are not generated by JETSET so the ρ^0 efficiency is assumed for these with correction factors $C = \varepsilon^i_{rec}/\varepsilon^{\rho^0}_{rec}$ $(i = f_0, f_2)$ being applied in the measured p_T and y intervals. Here, ε_{rec} is the efficiency for $\pi^+\pi^-$ pair reconstruction in the corresponding mass region.

To obtain the differential cross sections, the data sample is divided into 4 bins in rapidity and 7 bins in transverse momentum and the fit procedure is applied in each bin separately. The ρ^0 and $f_2(1270)$ resonance signals are clearly seen in all p_T intervals, while the $f_0(980)$ resonance is visible in the $\pi^\pm\pi^\mp$ spectra for $p_T < 1.5\,\mathrm{GeV/c}$ only. The first part of the error on the cross section represents the statistical error and is about 10%. The second part represents the quadratic sum of the systematic uncertainties. The major sources of systematic uncertainty arise from to the variation of the assumptions about the normalisation of the contribution of reflections in the fit procedure (up to 20%), the variation of the assumption about the f_0-meson width (up to 40% in the case of the f_0), the uncertainty in the detector acceptance and efficiency calculations (up to 13%) and the precision of the luminosity measurement (2%).

5 Discussion of results

In figure 4, the measured differential cross sections for inclusive photoproduction of the light resonances η, ρ^0, $f_0(980)$ and $f_2(1270)$ are presented as a function of rapidity and transverse momentum. Within the measured rapidity interval the resonance production rates are flat in rapidity, whilst the transverse momentum spectra follow a power law. Similar observations have already been made in charged particle production at HERA energies. A change from the exponential p_T spectra observed at lower energies to a power law is generally attributed to the onset

of hard parton scattering and has been successfully described by a thermodynamics-based approach [1]. It is interesting to note that both the large-p_T tail, where the hard parton scattering is expected to define the particle spectrum shape, and the low-p_T part of the spectrum, where the hadrons predominantly originate from the cascade decays of heavier resonances, are described with the same simple power law function. This, in addition to the intrinsic complexity of a hadronising partonic system, makes a thermodynamic analogy attractive also at high energies. A recently proposed generalisation of standard thermodynamics to non-extensive complex systems [2] leads to the appearance of a power-law energy distribution rather than a Boltzmann-like spectrum.

In figure 5, one of the universal features observed in the behaviour of long-lived hadrons [8] is investigated with the light resonances measured here. The double differential cross sections for η, ρ^0, $f_0(980)$ and $f_2(1270)$ production are presented as a function of $m + p_T$, where m is the meson's nominal mass. The cross sections follow closely the same power law function as that observed for pions at the same γp collision energy, once allowance has been made for the different isospin and spin of the various species of hadrons. Pion production has not been measured at HERA, so the pion results are derived from the measured charged particle spectrum by reducing this by 40% to account for the production of kaons, protons and long-lived charged leptons. The production rates for the measured hadrons are observed to depend primarily on variables such as the hadron's mass and transverse momentum rather than on their internal structure. This nontrivial fact supports a thermodynamic picture of particle production in high energy collisions. In addition, the observed regularity in the measured hadron spectra suggests a similar production mechanism for light long-lived hadrons, low mass vector mesons and orbitally excited tensor mesons.

The significant ρ^0 mass shift observed in this experiment and by the OPAL and DELPHI collaborations [15] requires further investigation. It is important to understand the origin of this effect in the context of the expected distortion of the nominal mass and width of hadronic resonances in heavy ion collisions at RHIC, where a similar effect could be attributed to the formation of a quark gluon plasma.

6 Summary

The first measurements of cross section for the inclusive photoproduction of the light resonances η, ρ^0, $f_0(980)$, and $f_2(1270)$ at a γp average collision energy of 210 GeV are reported. The measured differential spectra display features similar to those observed in studies of light, long-lived hadrons.

Acknowledgements

We are grateful to the HERA machine group whose outstanding efforts have made and continue to make this experiment possible. We thank the engineers and technicians for their work in constructing and now maintaining the H1 detector, our funding agencies for financial support, the DESY technical staff for continual assistance, and the DESY directorate for the hospitality which they extend to the non-DESY members of the collaboration.

References

[1] R. Hagedorn, Suppl. Nuovo Chimento **3**, (1965) 147.

[2] C. Tsallis, J.Stat.Phys. **52**, (1988) 479.

[3] C. Beck, Physica **A286**, (2000) 164.

[4] H.G. Sander, Nucl.Phys.Proc.Suppl. **71** (1999) 123.

[5] ZEUS Collab., M. Derrick *et al.*, Z.Phys. **C67**, (1995) 227.

[6] H1 Collab., C. Adloff *et al.*, Z.Phys. **C76**, (1997) 213.

[7] ZEUS Collab., J. Breitweg *et al.*, Phys.Lett. **B481**, (2000) 213 and **B401**, (1997) 192.

[8] A. Rostovtsev, In Proceedings of the 31st International Symposium on Multiparticle Dynamics (ISMD 2001), Datong, China, 1-7 Sep 2001.

[9] I. Abt *et al.* [H1 Collaboration], Nucl. Instrum. Meth. A **386**, (1997) 310 and 348.

[10] T. Sjöstrand, CERN-TH-6488 (1992), Comp. Phys. Commun. **82** (1994) 74.

[11] T. Sjöstrand, M. Bengtsson, Comp. Phys. Commun. **43** (1987) 367.

[12] R. Brun *et al.,* GEANT3 User's Guide, CERN-DD/EE/84-1.

[13] AFS Collab., T. Akesson *et al.*, Nucl.Phys. **B203**, (1982) 27.

[14] ALEPH Collab., D. Busculic *et al.*, Z.Phys. **C69**, (1996) 379.

[15] DELPHI Collab., P. Abreu *et al.*, Z.Phys. **C65**, (1995) 587. OPAL Collab., P. D. Acton *et al.*, Z.Phys. **C56**, (1992) 521.

[16] G. D. Lafferty, Z.Phys. **C60**, (1993) 659.

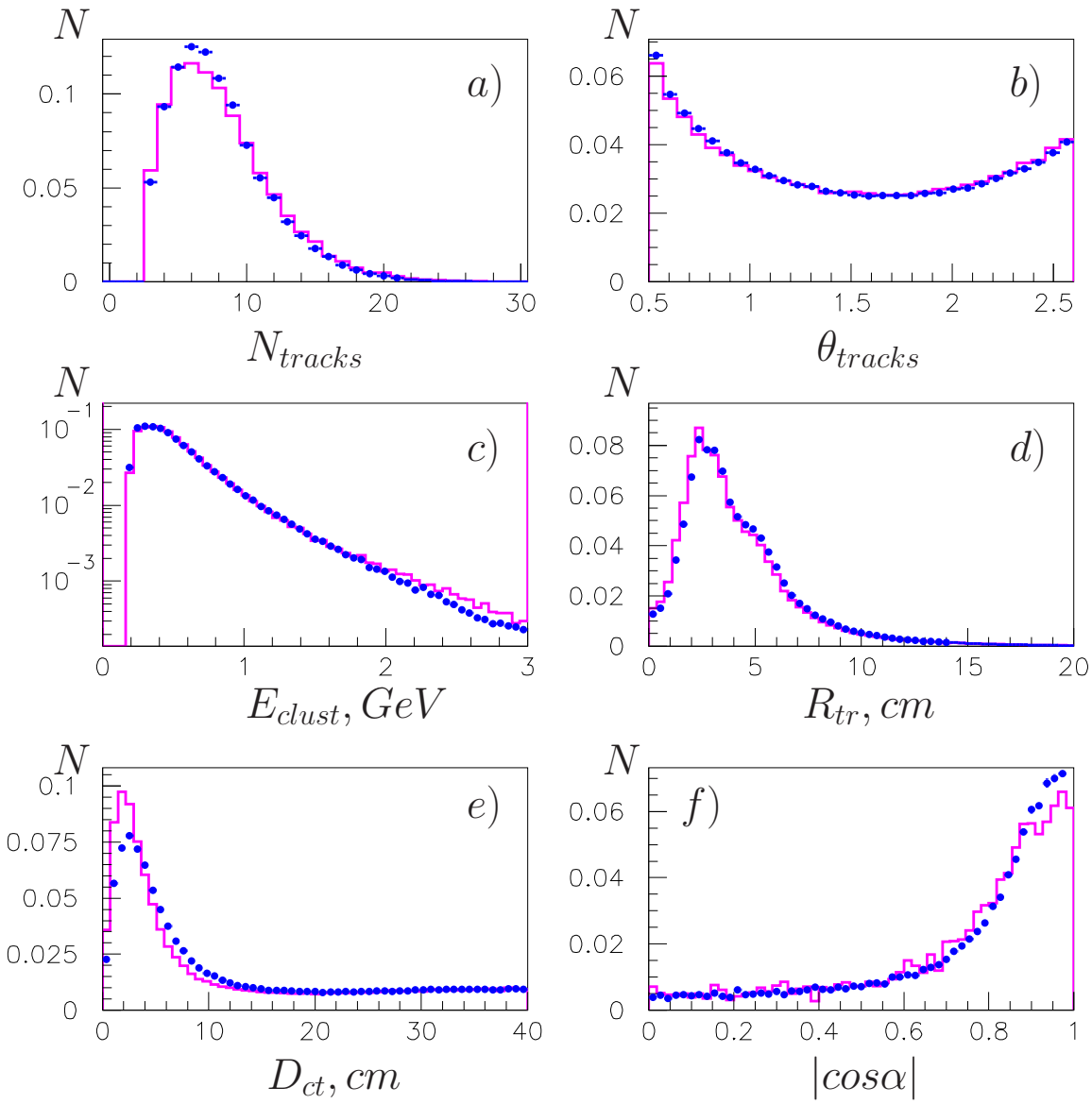

Figure 1: Comparison of various data and Monte Carlo distributions following the application of the selection criteria discussed in the text. The data and Monte Carlo distributions are normalized to the same area. a) Charged track multiplicity. b) Polar angle distribution of charged tracks. c) LAr cluster energy. d) Transverse radius of the clusters. e) Distance between cluster and closest track. f) $|\cos(\alpha)|$ distribution for electromagnetic cluster pairs with $p_T > 2\,\mathrm{GeV}$.

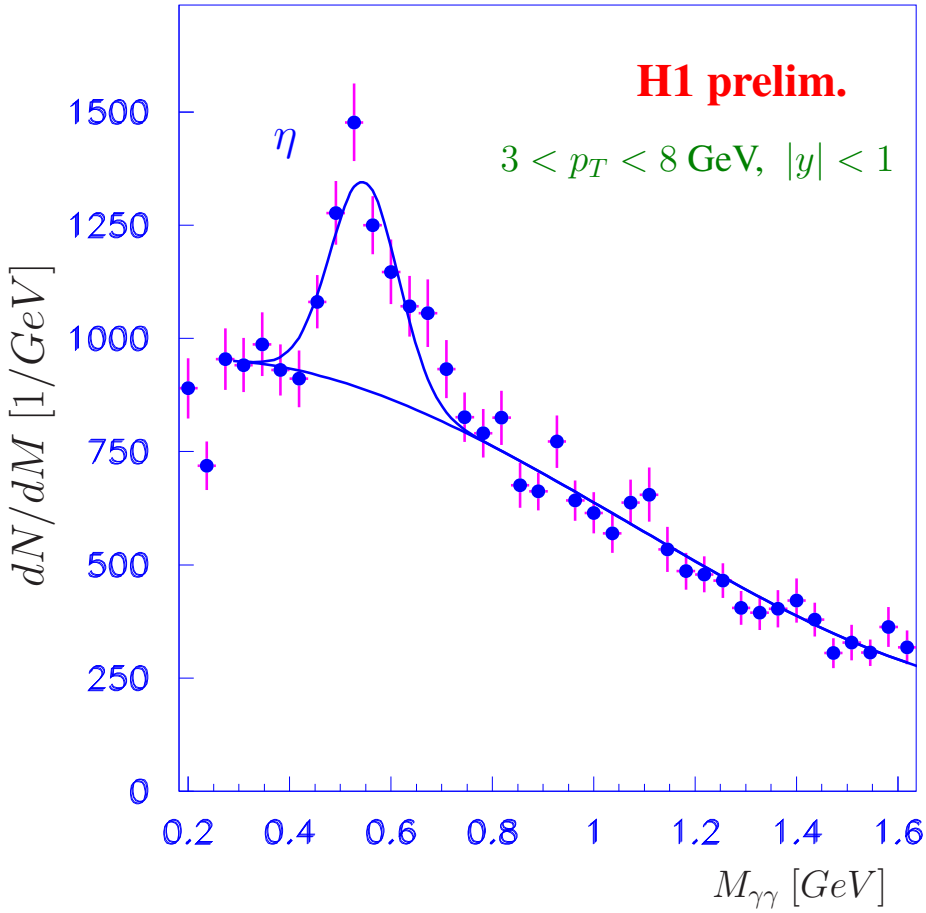

Figure 2: Two-photon mass spectrum after the application of the selection criteria discussed in the text. The smooth curve represents the result of a fit to the sum of a Gaussian and a third order polynomial.

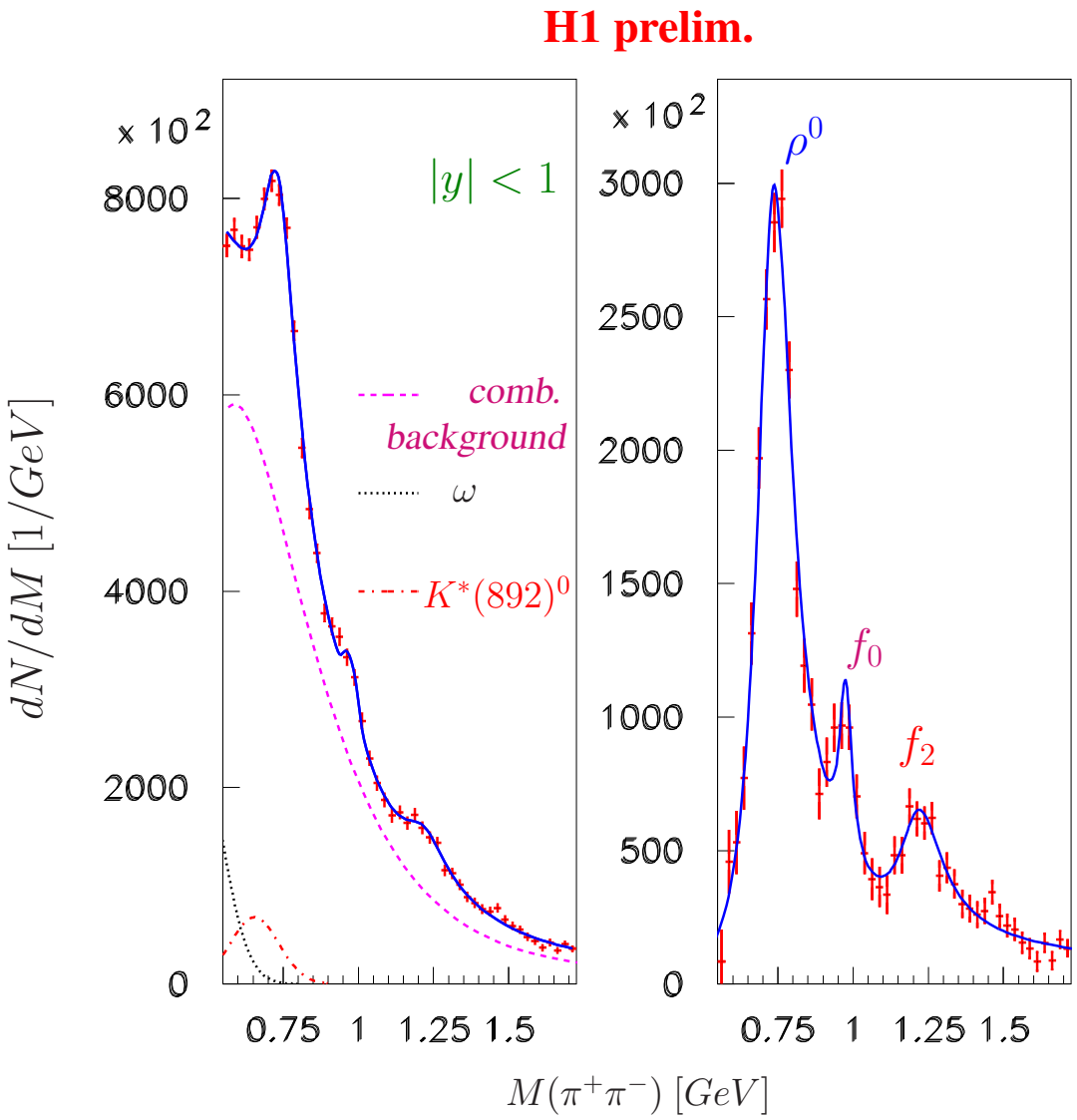

Figure 3: The $\pi^+\pi^-$ invariant mass spectrum following the subtraction of the like-sign spectrum. The full curve shows the results of the fit discussed in the text. In the left plot the dashed curve corresponds to the contribution of residual non-resonant background; the dotted and dash-dotted curves describe the contributions from ω and K^* reflections, respectively. In the right plot the points represent the data after subtraction of the background and the reflections.

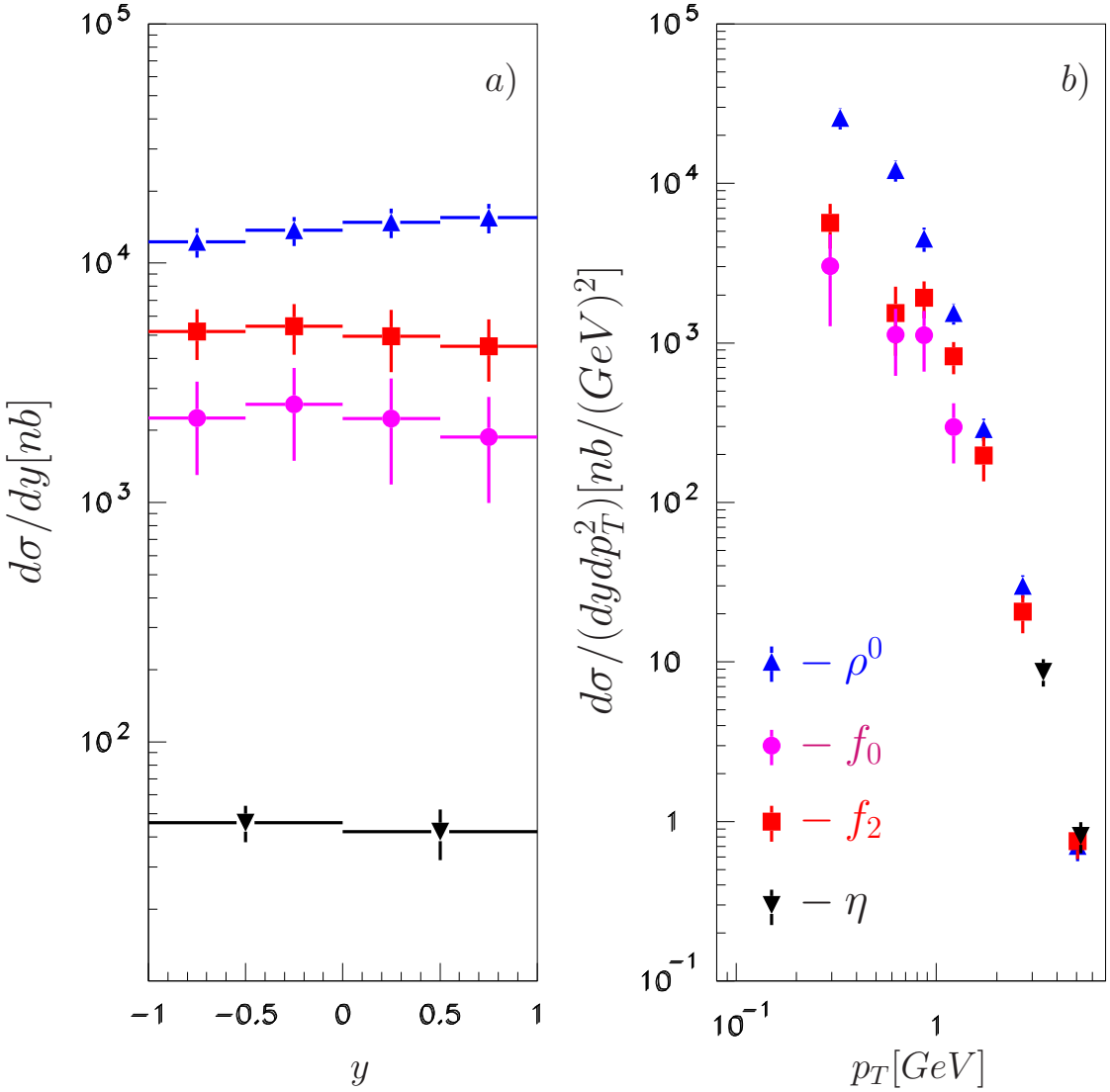

Figure 4: The differential photoproduction cross sections for η, ρ^0, $f_0(980)$ and $f_2(1270)$ mesons plotted as a function of (a) rapidity for $p_T > 0\,\text{GeV}$ (ρ^0, f_0 and f_2) and $3 < p_T < 8\,\text{GeV}$ (η) and (b) transverse momentum for $y_{lab} = 0$.

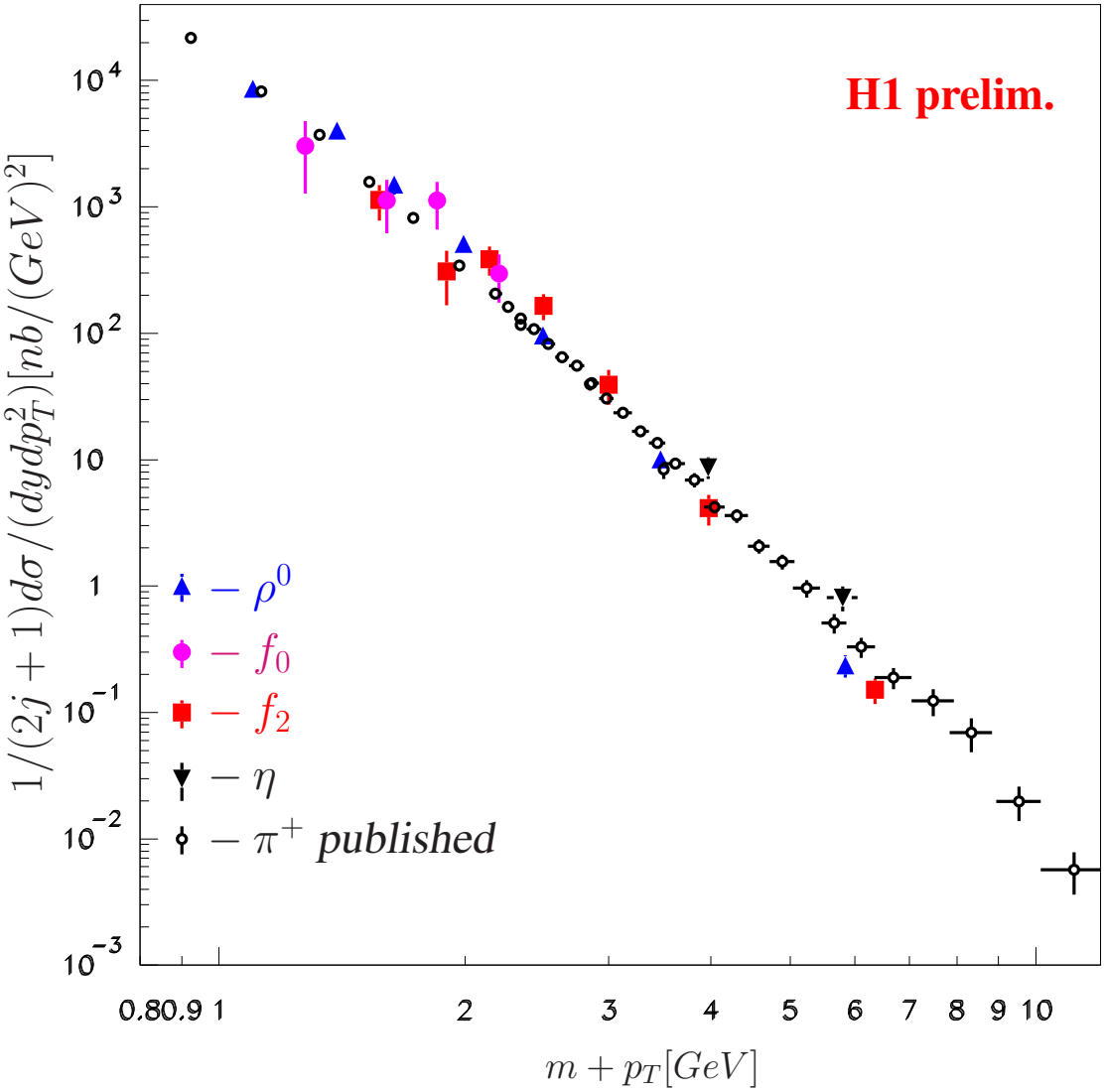

Figure 5: The differential photoproduction cross sections for η, ρ^0, $f_0(980)$ and $f_2(1270)$ mesons plotted as a function of $(m + p_T)$, with m being the nominal meson mass. The open symbols show the π^+ production cross section calculated from measurements of the charged particle spectrum in photoproduction.